IOP PUBLISHING JOURNAL OF PHYSICS D: APPLIED PHYSICS

J. Phys. D: Appl. Phys. **42** (2009) 185201 (9pp) doi:10.1088/0022-3727/42/18/185201

# Runaway-electron-preionized diffuse discharge at atmospheric pressure and its application

**E H Baksht, A G Burachenko, I D Kostyrya, M I Lomaev, D V Rybka, M A Shulepov and V F Tarasenko**

Institute of High Current Electronics, 2/3 Akademichesky Ave., Tomsk, 634055, Russia

E-mail: VFT@loi.hcei.tsc.ru

Received 3 April 2009, in final form 29 June 2009
Published 24 August 2009
Online at stacks.iop.org/JPhysD/42/185201

**Abstract**

The paper presents the results of experimental research on nanosecond high-pressure diffuse discharges in an inhomogeneous electric field with a time resolution of ∼100 ps. It is shown that decreasing the voltage pulse duration enhances the feasibility of the diffuse discharge with no additional ionization. In particular, with a narrow interelectrode gap, a diffuse discharge in atmospheric pressure air with preionization by runaway electrons, called a runaway-electron-preionized (REP) diffuse discharge (DD), was realized. It is found that most of the energy is deposited to the REP DD plasma once the voltage across the gap reaches its maximum. It is demonstrated that the REP DD holds promise for producing high-power VUV pulses. The radiation power attained with xenon at a wavelength of ∼172 nm is 8 MW. The treatment of an AlBe foil with an REP DD in atmospheric pressure air provides cleaning of its surface layer from carbon and penetration of oxygen atoms into the foil to a depth of 450 nm per 300 pulses.

## 1. Introduction

Nowadays, high-pressure pulsed diffuse discharges find wide application in science and technology, in particular in designs of gas and plasma lasers [1–3]. Diffuse discharges are produced using various preionization sources and discharge gaps with a homogeneous electric field. Since the late 1960s, the initiation of atmospheric-pressure diffuse discharges in various gases has been known to be possible even with no additional preionization [4, 5], for which short high-voltage pulses and discharge gaps with a cathode of small curvature radius are used. Atmospheric-pressure diffuse discharges were obtained in helium [4], in air [5] and later in $SF_6$ [6]. A peculiar feature of this discharge type is the generation of x-rays [4, 5] and runaway electron beams [7, 8–25]. Before 1990, there had been many papers devoted to x-ray and e-beam generation in nanosecond diffuse discharges [8]; however, since that time interest in this field has been lost. Apparently, this is due to the subnanosecond time of the processes occurring in the runaway-electron-preionized diffuse discharge (REP DD) gap and thus to the complexity of nanosecond and subnanosecond high-voltage pulsers and measurements of discharge and runaway e-beam characteristics. A review of relevant studies conducted till 2003 is summarized in [8]; however, in the studies, the time resolution of measurements was about a mere 1 ns, the voltage pulse duration ranged over several nanoseconds and the mechanism of diffuse discharges was not made clear. The author of [8] supposed that the diffuse discharge is due to gas preionization by runaway electrons with an 'anomalous' energy $T$ ($T > eU$, where $U$ is the voltage across the gap) produced at the streamer head near the cathode.

In the past five years, interest in this discharge mode has been rekindled [9–25]. It was found that atmospheric-pressure discharges in an inhomogeneous electric field feature a number of unique properties; in particular the specific input power can reach ∼1 GW cm$^{-3}$ (∼800 MW cm$^{-3}$ at the gap centre [10, 11]). Another peculiarity of the REP DD is that its ignition is slightly affected by the polarity of a nanosecond voltage pulse [12–14]. A diffuse discharge with a voltage rise time of several nanoseconds was obtained in [10] and of tens of nanoseconds in [14, 15], and a diffuse discharge with a voltage of tens of kilovolts was realized in [10, 18]. In the batch mode,

 

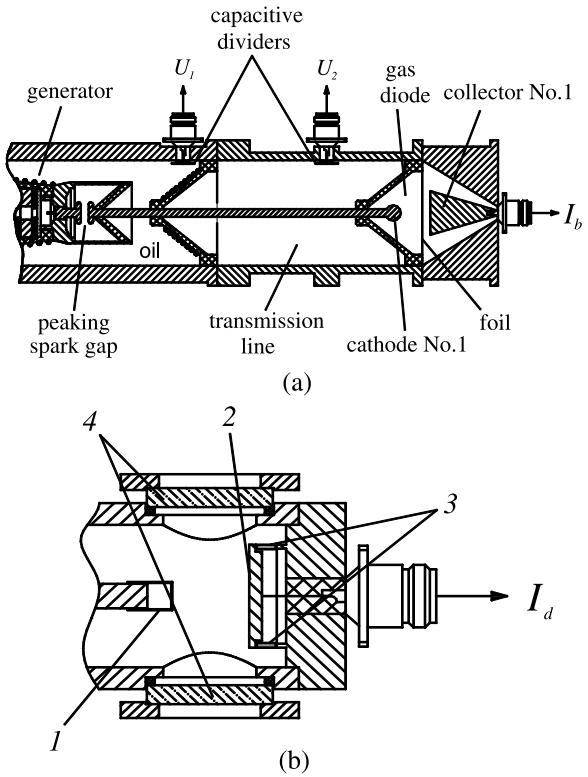


**Figure 1.** Schematic of pulser with a collector (*a*); discharge chamber (*b*): 1—cathode, 2—anode, 3—current shunt, 4—windows.

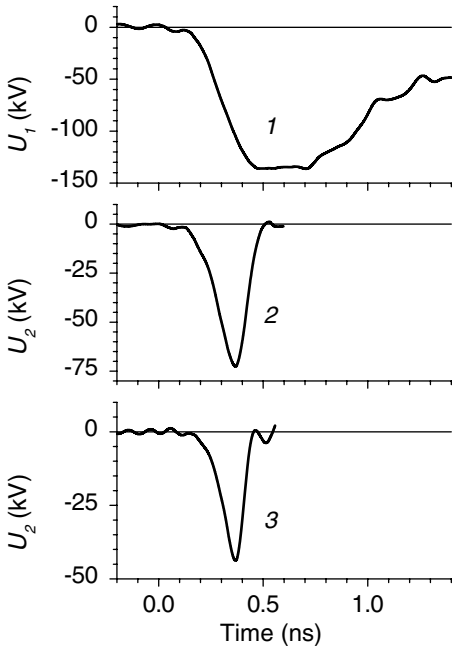


**Figure 2.** Waveforms of the incident voltage wave from the capacitive dividers located at the SLEP-150 output ($U_1$) and in the transmission line downstream of the closing switch ($U_2$): incident voltage wave across the closing switch (1); incident voltage wave downstream of the closing switch for a gap of 3 mm (2) and 1 mm (3).

the REP DD retained its properties at high pulse repetition frequencies, e.g. up to 3 kHz [19]. The REP DD plasma was used to design VUV sources [16, 17] as well as to modify and clean the surface of Cu foils [20]. However, this discharge type is still poorly understood primarily due to the short duration of the initial discharge phase responsible for its diffuse character.

The objective of this work was to investigate the conditions and the properties of subnanosecond (up to ∼100 ps) and nanosecond REP DD and to demonstrate the applicability of this discharge type. In the experiments, the time resolution of a measuring system was ∼100 ps.

## 2. Experimental procedure and equipment

The discharge parameters (current–voltage characteristics, space form and radiation spectra) were studied on RADAN-220 and SLEP-150 pulsers. Figure 1 shows a pulser with a collector (*a*) replaceable by a discharge chamber (*b*). The inner diameter of the gas discharge chamber was ∼50 mm. Cathode 1 of small curvature radius and plane anode 2 ensured field amplification near the cathode. The cathode was either a steel sphere of diameter 9.5 mm or a steel foil tube of diameter ∼6 mm and thickness 100 $\mu$m. The plane anode was a brass plate connected to the chamber case with shunt 3. In the studies, foil and grid anodes were also used. With the foil anode, the characteristics of a supershort avalanche electron beam (SAEB) [24] were measured on the collector placed downstream of the foil. A more detailed description of studies on SAEBs can be found in [24, 25]. With the grid anode, images of the discharge glow in the gap were taken from the right end face of the electrode, and the displacement current proportional to that through the gap was measured with the collector. The interelectrode gap was between 0 (short-circuit) and 19 mm. Further increasing the interelectrode gap width resulted in a complete breakdown over the insulator surface of the discharge chamber.

In experiments with short voltage pulse durations, the SLEP-150 nanosecond pulser was used [26]. The pulser produced voltage pulses of amplitude up to 150 kV (across a high-resistance load) with a voltage rise time of ∼0.3 ns. At the output of the SLEP-150 pulser, there was a transmission line. When filled with transformer oil and air, the transmission line had an impedance of 100 Ω and 140 Ω, respectively. The voltage pulse FWHM in the transmission line of the SLEP-150 pulser was variable between 1 and 0.1 ns because of a closing switch located at the input of the air-filled transmission line. In a number of experiments, the FWHM was ∼2 ns at a voltage pulse amplitude of ∼150 kV. Figure 2 shows waveforms of the voltage pulses with and with no closing switch. With the closing switch, its gap was 3 and 1 mm. With a voltage pulse of FWHM ∼0.1 ns, the voltage rise time also approximated 0.1 ns and the voltage pulse amplitude was ∼45 kV (figure 2, curve 3). The RADAN-220 pulser [27] had an impedance of 20 Ω. The pulser produced a voltage pulse of amplitude ∼250 kV and FWHM ∼2 ns (with a matched load) in the discharge gap at a voltage rise time of ∼0.5 ns. Both the setups ensured a possibility to reverse the voltage polarity across the electrode of small curvature radius.

The voltage pulses were measured with capacitive voltage dividers and the discharge current $I_d$ was measured with the shunt 3 (figure 1(*b*)) composed of low-impedance chip

resistors. The signals from the shunt, capacitive dividers and collectors were recorded by 20 GS/s TDS-6604 and 25 GS/s DPO70604 oscilloscopes both with a 6 GHz band. The sensors and the oscilloscopes were connected through pulse coaxial cables and Barth Electronics 142-NM attenuators. Images of the integral discharge glow were taken through a grid or a window using a SONY A100 camera. The x-ray exposure dose was measured using an Arrow-Tech dosimeter (Model 138) sensitive to x-rays with a quantum energy greater than 16 keV. The dosimeter was installed 0.1–3 cm away from the foil plane and perpendicular to the cathode axis. The x-ray pulse shape was recorded by a diamond detector with a time resolution of ∼0.2 ns.

## 3. Discussion of experimental results

As noted above, for the ignition of an REP DD, nanosecond high-voltage pulses must be applied to the gap with an inhomogeneous electric field. The voltage pulses produced by the pulsers across the matched load had an FWHM of ∼2, ∼1, ∼0.2, ∼0.15 and ∼0.1 ns. However, the actual duration of the discharge current pulse was normally greater than the duration of the voltage pulse across the matched load due to the inductance of the peaking spark gap and varying impedance of the gas discharge plasma during its breakdown. Figure 3(*a*) shows the waveforms of the voltage across the gap and of the discharge current at a voltage pulse duration of ∼2 ns and an amplitude of ∼150 kV [22]. The gas discharge chamber was filled with $SF_6$ at atmospheric pressure and a volume discharge was ignited. It is seen that the discharge current arises during the voltage rise and its polarity does not reverse. More than 80% of the energy stored in the pulser is deposited to the discharge plasma in ∼3 ns. The first peak of the discharge current on the initial portion of its waveform is due to the displacement current through the gap. The third peak of current and the second peak of voltage are due to the reflection of the voltage pulse from the discharge gap and then from the opposite end of the high-voltage line of the pulser and its return to the discharge gap. For the REP DD in $SF_6$, the impedance of the discharge plasma was greater than that of the pulser.

In air and nitrogen as well as in inert gases, the impedance of the discharge plasma during the breakdown decreases much faster than that in $SF_6$, and the current of the diffuse discharge is oscillatory. Figure 3(*b*) shows a waveform of the discharge current pulse in atmospheric pressure nitrogen with a 16 mm interelectrode gap and RADAN-220 pulser. The reverse of the voltage pulse polarity across the electrode of small curvature radius slightly affects the ignition of the REP DD, which agrees with the results obtained earlier [12–14]. A waveform of the discharge current rise for the conditions of figure 3(*b*) and a waveform of the SAEB current downstream of the AlBe foil are shown in figure 3(*c*). The SAEB appears within ∼600 ps after the application of the voltage pulse from the RADAN-220 pulser.

The images of the discharge glow with a negative voltage pulse across the electrode of small curvature radius for the RADAN-220 and SLEP-150 pulsers are shown in figures 4 and 5, respectively. Bright spots are normally evident only

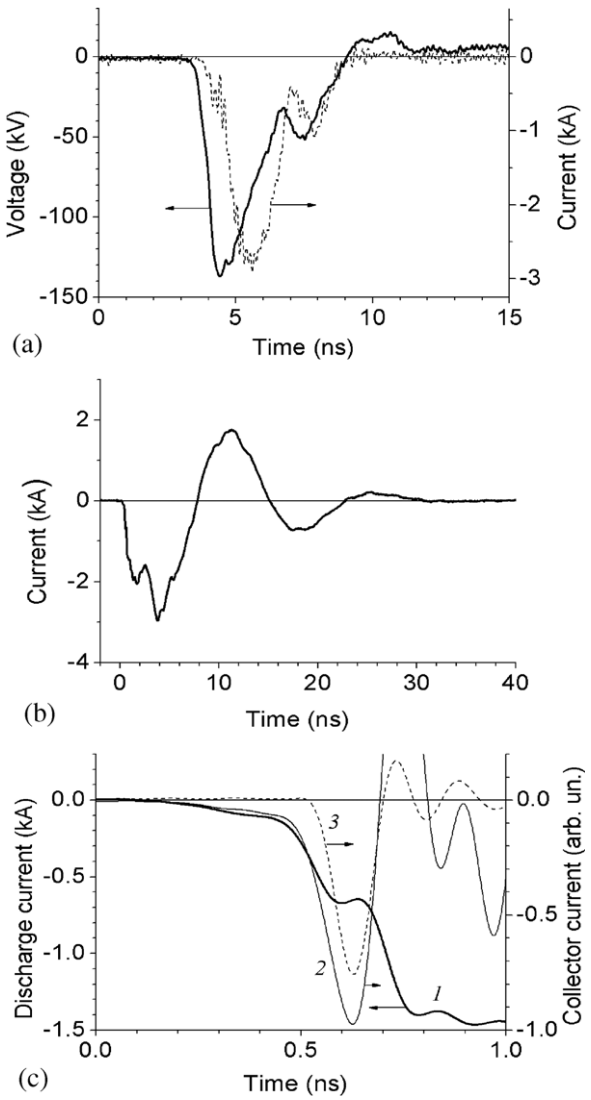


**Figure 3.** Waveforms of the voltage across the gap and discharge current (*a*), discharge current from the shunt ((*b*) and (*c*), curve 1), electron beam current and displacement current ((*c*), curve 2), electron beam current downstream of the AlBe foil measured by the collector with the highest time resolution of the oscilloscope ((*c*), curve 3). The pulser is RADAN-220, the anode–cathode spacing is 16 mm, curves 1, 2 and 3 are synchronized.

at the cathode (figures 4(*a*)–(*c*) and 5). As the pressure increases, the cross-section of the discharge region with a bright glow decreases (figure 4(*c*)). Under these conditions, the comparatively large interelectrode gaps of the discharges in atmospheric pressure nitrogen, air, $SF_6$ and other gases ensured a diffuse discharge with the longest voltage pulse durations of the pulser (∼2 ns at the matched load) and maximum amplitudes (∼250 kV). The probability of discharge constriction increased with increase in the voltage pulse duration and rise time, decreasing the interelectrode gap width, and increasing the gas pressure in the discharge chamber. Note that for the RADAN-220 pulser with a large specific energy deposition (∼1 J cm$^{-3}$), the constriction of the discharge occurred, and as the pressure was decreased down to tenth to hundredth of fractions of atmosphere, the REP-to-spark discharge transition took place.

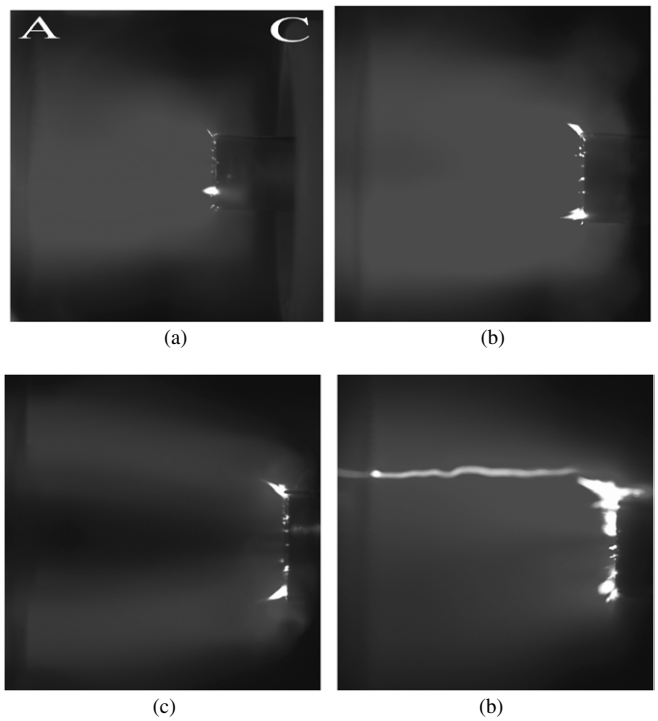


**Figure 4.** Images of the discharge glow in nitrogen ((*a*)–(*c*)) and air (*d*) with an anode–cathode spacing of 14 mm. The pulser is RADAN-220, the pressure is 0.5 (*a*), 1 ((*b*), (*d*)) and 3 atm (*c*).

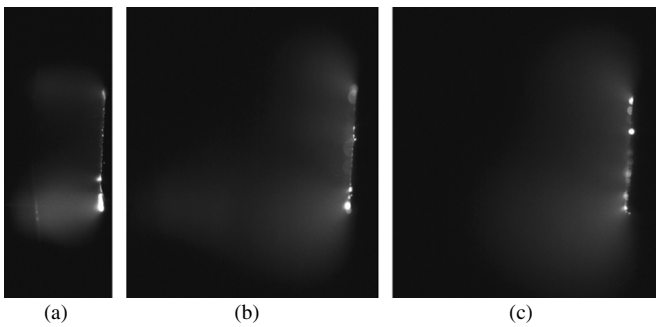


**Figure 5.** Images of the discharge glow in air with an anode–cathode spacing of 4 (*a*), 12 (*b*) and 16 mm (*c*). The pulser is SLEP-150, the pressure is 1 atm.

The REP DD is easiest to initiate in light gases (helium, hydrogen and neon) at high pressures. We obtained a discharge in helium with the RADAN-220 pulser at a pressure of up to 15 atm. The constriction of the discharge in air occurs earlier than that of the discharge in nitrogen. It is seen in figure 4(*a*) that in the diffuse discharge in atmospheric pressure air with a 14 mm gap, a brighter channel appears, whereas in the discharge in nitrogen at a pressure of 1 and 3 atm with the same gap width, no discharge constriction is observed. With the RADAN-220 pulser, decreasing the gap width to 4 mm ensured constriction of the atmospheric-pressure discharges in $SF_6$, air and nitrogen. As the interelectrode gap width was decreased, the breakdown voltage of the discharge gap decreased, which follows from the right branch of the Paschen curve for nanosecond voltage pulse durations [8, 15]. For the constricted discharge, the number of oscillations per current

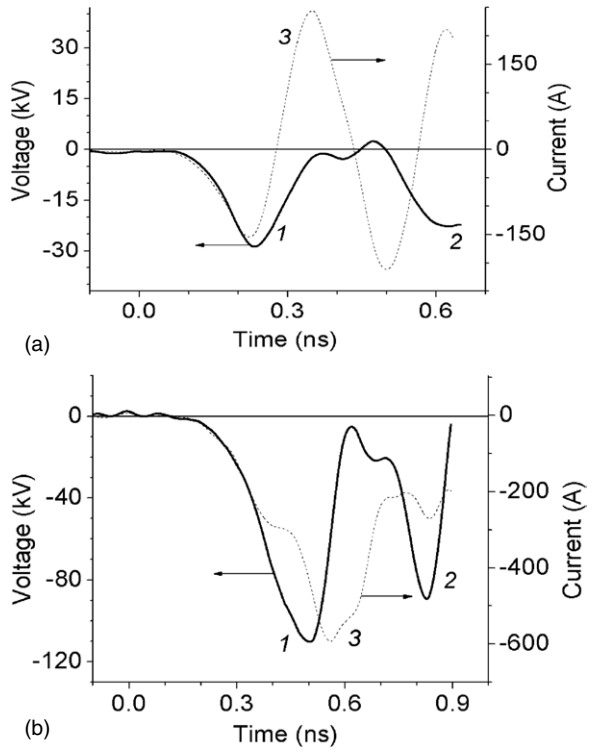


**Figure 6.** Waveforms of the voltage (incident wave 1 and reflected wave 2) and discharge current 3 with the displacement current at a voltage pulse FWHM of 0.1 ns (*a*) and 0.2 ns (*b*). The pulser is SLEP-150, the air pressure is 1 atm, the anode–cathode spacing is 12 mm.

pulse and hence the duration of the discharge current pulse increase.

Decreasing the voltage pulse duration considerably enhances the feasibility of a diffuse discharge. Figure 5 shows the images of the discharge glow in air for a voltage pulse duration of ~0.2 ns in the transmission line and different interelectrode gaps. Because of the decrease in the voltage pulse duration, no constriction of the discharge in atmospheric pressure air was observed with a 4 mm interelectrode gap. With $d = 16$ mm, the REP DD had no time to develop and the discharge glow was observed only at the cathode, which corresponded to a pulsed corona discharge. However, cathode spots did have a chance to develop in this mode. On a pulser similar to SLEP-150, the transition to a corona discharge within ~2 ns after the ignition of a diffuse discharge was observed only with a large (67 mm) interelectrode gap [14].

The experiments suggest that with applied voltage pulses of long duration and steep rise, the REP DD is the initial stage of a spark discharge. However, as the voltage pulse duration is increased, the diffuse stage of the REP DD, as a rule, escapes detection due to the high radiation intensity of the constricted discharge.

Figure 6 shows waveforms of the voltage pulse (incident wave 1 and wave reflected from the gap 2) and discharge current 3 with the displacement current during the voltage rise for a 12 mm gap. It is seen that with subnanosecond voltage pulses, a change in the discharge mode is observed. For a voltage pulse FWHM of <0.2 ns (figure 6(*a*)), the displacement current appears during the voltage rise. Under

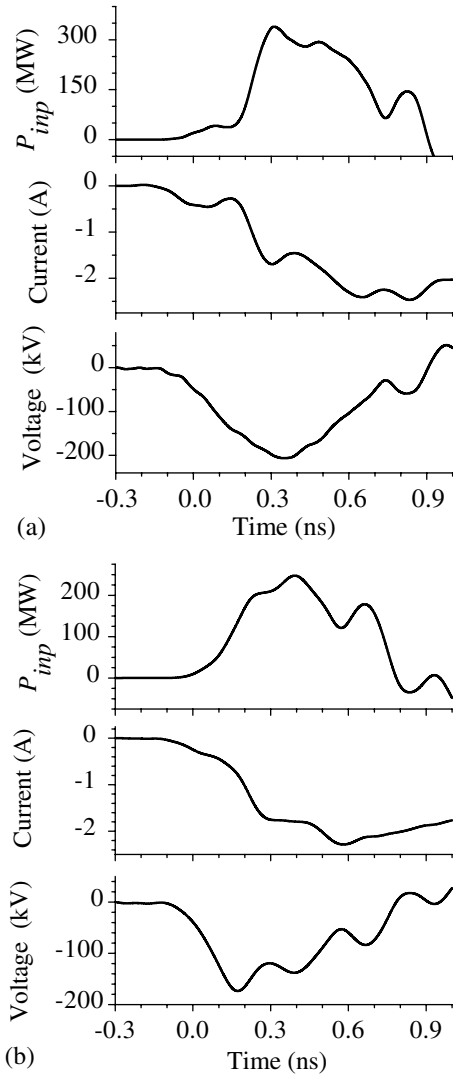


**Figure 7.** Synchronized waveforms of the voltage and discharge current, and calculated input power: spherical (*a*) and tubular (*b*) cathode. The pulser is SLEP-150, the air pressure is 1 atm, the anode–cathode spacing is 12 mm.

these conditions, the discharge glow corresponds to a pulsed corona discharge (figure 5(*c*)). For a voltage pulse FWHM of $\geqslant$0.2 ns, the discharge current increases within 300 ps after the beginning of the pulse (figure 6(*b*)) and this is due to the ionization processes occurring across the whole gap width after its bridging by the ionization wave [29]. In this case, the gap glow corresponds to a REP DD (figures 5(*a*) and 4(*a*)–(*c*)). Thus, decreasing the voltage pulse duration and amplitude makes a discharge mode possible in which the ionization wave front reaches the anode at the instant the voltage across the gap vanishes.

Figure 7 shows time-synchronized waveforms of the voltage and discharge current, and calculated input power at a voltage pulse FWHM of ~1 ns in the transmission line of the SLEP-150 pulser for two different cathodes. The current and voltage waveforms are synchronized to no worse than 50 ps. The recording of the incident and reflected voltage waves made it possible to determine the gap voltage during the first 900 ps of the discharge development. One can distinguish two stages of the discharge: a stage before the maximum voltage across the gap and a stage after the voltage maximum. The voltage drop across the gap is due to the arrival of the dense plasma front at the anode and to the development of ionization processes in the gap. It is possible to roughly estimate the energy deposition to the gas before the gap is bridged by the ionization wave. This energy was ~50 mJ and ~30 mJ for the spherical and tubular cathodes, respectively. The actual energy deposition at this discharge stage was smaller since the total input power is made up not only by the active component, but also by the reactive component.

Most of the energy is deposited to the discharge plasma once the voltage across the gap reaches its maximum, and this energy can be determined with a reasonable accuracy because the entire gap is filled with the plasma. Calculations show that once the voltage across the gap reaches its maximum, about 100 mJ is deposited to the discharge plasma within 900 ps after the beginning of the voltage pulse with both cathodes. With the tubular cathode, the time for which it was possible to determine the energy deposition was 530 ps due to the faster voltage drop across the gap and with the spherical cathode it was 350 ps. Under these conditions, the specific input power is hundreds of megawatts per cubic centimetre. The volume filled with the dense plasma is typically less than 1 $cm^3$ and hence the average specific power density of energy deposition in atmospheric pressure air for the tubular cathode $>$200 MW $cm^{-3}$ (figure 7(*b*)).

With the RADAN-220 pulser, the specific energy deposited in the REP DD in air reached ~1 J $cm^{-3}$ and the specific input power density was ~0.8 GW $cm^{-3}$. Most of the energy ($>$90%) was deposited on the arrival of the ionization wave front at the anode. Once the voltage across the gap reaches its maximum, the discharge mode corresponds to an anomalous pulsed glow discharge, except for one distinction. The distinction is that the current from the cathode is mainly due to explosive emission. As indicated above, almost in all gases the REP DD features bright spots at the cathode. These spots result from explosive electron emission [30]. Note that in some gases, e.g. in helium and nitrogen, the REP DD can involve other mechanisms of electron emission from the cathode. In the REP DD in nitrogen, a diffuse glow with no cathode spot is observed near the side surface of the cathode (figures 4(*a*)–(*c*)). Apparently, the electron emission in this cathode region is ensured by ions and photons of the VUV range. With the RADAN-220 pulser, a REP DD in helium with no cathode spot was realized at a pressure of ~0.01 atm (see figure 4(*a*) in [23]).

## 4. Radiation in the REP DD

The REP DD plasma is a source of x-rays and runaway electron beams and of optical radiation in different spectral ranges [4–26, 28]. In our work, we measured, in addition to the discharge parameters, the SAEB and x-ray characteristics downstream of the foil. The discharge plasma was a source of high-power spontaneous radiation. With the RADAN-220, the maximum amplitude of the beam current downstream of an Al foil 10 $\mu$m thick was ~50 A, and with the SLEP-150 pulser it was ~25 A.

In the measurements, the beam current FWHM was ∼100 ps over the entire foil surface (figure 3(*c*)). With the maximum resolution of the measuring system, the SAEB pulse duration measured over a small foil area was 80 ps. Under optimum conditions, the delay time between the SAEB pulse generation and the beginning of the voltage rise was 300–500 ps. With the RADAN-220 pulser, the x-ray exposure dose downstream of a Cu foil 20 $\mu$m was ∼1.5 mR, and with the SLEP-150 pulser it was ∼0.6 mR. The x-ray pulse from the discharge chamber was ∼0.2 ns at FWHM, which corresponds to the maximum resolution of the diamond detector. Detailed studies of SAEBs and x-rays are reported in [18, 19, 22–25, 28].

With the RADAN-220 pulser and the discharge chamber shown in figure 1, the total radiation power density of Xe dimers was ∼1 MW cm$^{-3}$ at a wavelength of ∼172 nm. Unlike the radiation power of Xe dimers, the radiation powers of Kr dimers ($\lambda \sim 146$ nm) and Ar dimers ($\lambda \sim 126$ nm) under the same conditions were 1.5 and 2 times lower, respectively. At a pressure of 1.2 atm, the radiation pulses of Xe, Kr and Ar dimers were ∼140 ns at FWHM. As the Xe pressure was increased to 12 atm, the FWHM decreased to 8 ns. In the REP DDs in nitrogen and air (as well as in $SF_6$ due to the nitrogen additive), the bands of the second positive nitrogen system feature the highest power (the most intense line is at 337.1 nm). With the RADAN-220 pulser, the radiation power of the second positive nitrogen system was 120 kW to a solid angle of $4\pi$, which is three times greater than that obtained in [10]. The radiation pulse, in this case, was 4 ns at FWHM.

## 5. Mechanisms of the REP DD ignition

We think that under the experimental conditions, the dynamics of the diffuse discharge in the gap with one electrode of small curvature radius is the following. The highest electric field arises near the electrode of small curvature radius due to microirregularities. With a negative high-voltage pulse, the electric field is amplified at the cathode resulting in field emission from the cathode [6]. The field emission is enhanced due to the positive charge of the ions produced near the cathode [23]. A part of the field emission electrons in the near-cathode region with a high electric field passes into the runaway mode. The energy gained by these fast electrons is greater than that corresponding to the maximum ionization cross-section. The electrons move towards the anode and preionize the gas. Because of the field amplification near the cathode and increased voltage across the gap, the fast electrons can be accelerated to energies of several kiloelectronvolts and, with high $E/N$ ($E$ is the electric field strength, $N$ is the gas concentration), to tens of kiloelectronvolts. However, with distance from micro- and macroirregularities, the electric field decays rapidly and the energy of the fast electrons, as a rule, decreases to several electronvolts.

The electrons produced near the cathode due to ionization by fast electrons give rise to electron avalanches. The number of initial electrons from which the avalanches evolve is so high that the heads of the electron avalanches are overlapped before a streamer starts to develop. The high density of the initial electrons and the overlapping of the electron avalanche heads are due to the ignition of a diffuse discharge in a wide range of experimental conditions. Thus, comparatively dense diffuse plasma is produced near the cathode during the voltage rise (see the image in figure 5(*c*) for a short pulse duration and oscilloscope traces in figure 6(*a*)). With a rather high electric field in the gap, as is normally the case under the above conditions, the plasma front moves towards the anode. We suppose that once the plasma is produced near the cathode, a part of the electrons can be additionally accelerated due to polarization self-acceleration of the electrons and this is assisted by the increase in voltage across the gap. Note that polarization self-acceleration of electrons at the 'polarization streamer front' was predicted earlier in [31]. Under the above conditions, the electrons at the front of the diffuse discharge plasma expanding from the cathode are accelerated both by the increase in voltage across the gap and by the excess (uncompensated) negative charge in the heads of electron avalanches. Moreover, the electric field in the gap is further increased because it is forced out from the dense plasma of the ionization wave. All these lead to the generation of runaway electrons in the gap. These electrons cross the rest of the gap ensuring its preliminary ionization and hence the ignition of diffuse discharge.

Thus, the generation and the runaway of field emission electrons due to both the external field and the positive ion charge near the cathode provide a diffuse discharge in the near-cathode region at increased pressures. The runaway electrons produced in the gap preionize the rest of the gap through polarization self-acceleration. It should be noted that the increase in $E/N$ both by decreasing the gap pressure and by increasing the voltage pulse amplitude and, in some cases, by decreasing the gap width may provide continuous acceleration of the electrons emitted from the cathode. In this case, the duration and rise time of the beam current pulse normally increase [18, 23]. Figure 3(*c*) shows the waveforms of the discharge current, displacement current from the collector with the runaway electron current downstream of the grid and the runaway e-beam current downstream of the foil. The gap was filled with atmospheric pressure air. It is seen that once the beam current arises, the discharge current increases again, which corresponds to the waveform of the discharge current in figure 6(*b*).

The ignition of a diffuse discharge with a positive polarity across the electrode of small curvature radius is also associated with the generation of runaway electrons. However, under these conditions, the gap is preionized mainly by x-ray quanta resulting from deceleration of runaway electrons at the anode and in the gap. In the regions of maximum field strength (electrode of small curvature radius), a part of the initial electrons turns to the runaway mode. The runaway electrons move towards the anode and, when decelerated at the anode, produce x-ray quanta that preionize the gap. With a positive polarity, runaway electrons are generated in a rather narrow region near the anode in which the electric field amplification is pronounced. Therefore, the energy of x-ray quanta is much lower than that with a negative polarity of the electrode of small curvature radius. Once the dense plasma is produced near the anode, its front propagates towards the cathode and

the field critical for runaway of electrons is achieved at the ionization wave front. In our experiments and in [5], x-rays were recorded both with negative and positive polarity of the electrode of small curvature radius. However, because of the smaller energy of x-ray quanta with a positive polarity of the electrode of small curvature radius, they are more difficult to record. With a negative polarity, x-rays also participate in the preionization of the gap; however, the runaway electrons have a dominant role in the process.

Thus, the diffuse discharge features stable ignition in different atmospheric-pressure gases with nanosecond high-voltage pulses and rather large gaps (several centimetres) with no additional preionization source. The ignition of the diffuse discharge in the gap with an inhomogeneous electric field is due to the preionization of the gap by the fast electrons resulting from field amplification at the cathode and in the gap as well as by the x-ray quanta produced on deceleration of the runaway electrons at the electrode and in the gas. By increasing the voltage pulse duration and rise time, the gas pressure, the specific energy deposition, etc, cause constriction of the REP DD and REP-to-spark discharge transition.

In [9], it was proposed to name this discharge mode as a volume discharge initiated by an avalanche electron beam (VDIAEB). Because the abbreviation VDIAEB is somewhat awkward and is difficult to pronounce in English, we will call this discharge mode as a REP DD, i.e. a diffuse discharge with preionization by runaway electrons, or a runaway-electron-preionized diffuse discharge. The REP DD can find wide application in different fields. In the next section, we briefly describe two possible applications of REP DDs in various gases at a pressure of ∼1 atm.

## 6. Application of the REP DD

### 6.1. VUV and UV excilamps

The REP DD can be used in designs of high-power excilamps. Preliminary studies show that the highest radiation power is attained in inert gases [16, 17]. Relatively high radiation powers are obtained in mixtures of inert gases with halogenides [32]. Figure 8 shows the design of a gas discharge chamber connected to a pulser with an impedance of 10 Ω. The voltage pulse duration of the pulser at a matched load was 50 ns. With this setup, the Xe discharge had the shape of a truncated cone with the base on the anode. The diameter of the emitting region (the discharge plasma) was ∼6 cm near the cathode and ∼8 cm near the grid anode, and the interelectrode gap was 4.5 cm. Studies show that in this setup, the radiation power of Xe dimers increases with increasing xenon pressure up to 1 atm (figure 9). The maximum radiation power of $Xe_2^*$ dimers to a full solid angle was ∼8 MW at 140–200 nm. The radiation pulse was no greater than ∼100 ns at FWHM and the radiation power density was $\sim 2 \times 10^4$ W cm$^{-2}$ with an excitation pulse of tens of nanoseconds. A similar value of the radiation power was attained before only with inert gases pumped by electron beams [1–3].

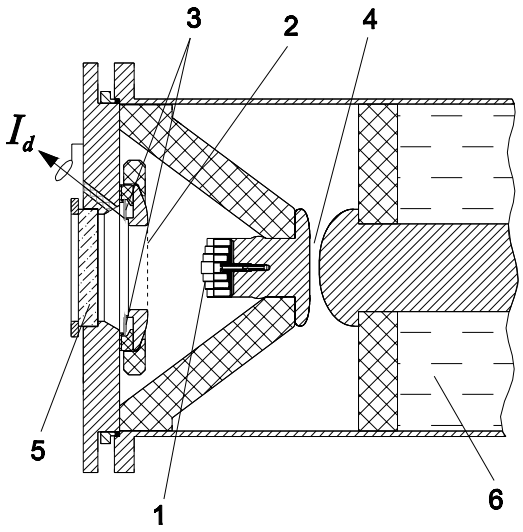


**Figure 8.** Schematic of the discharge chamber: 1—cathode, 2—grid anode, 3—current shunt, 4—peaking spark gap, 5—window, 6—transformer oil.

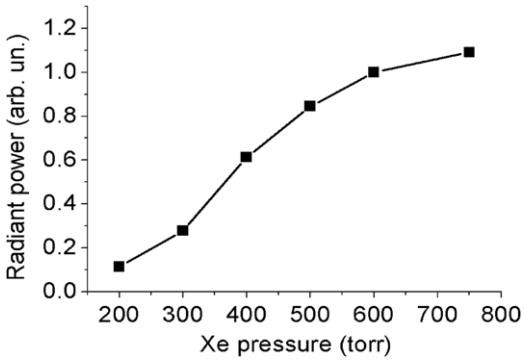


**Figure 9.** Pressure dependence of the $Xe_2^*$ output power.

### 6.2. Modification and cleaning of metal surfaces

The REP DD is characterized by high specific input powers. Moreover, the plasma of the discharge is a high-power UV and VUV source and generates a runaway electron beam and a shock wave [20–24]. These properties of the REP DD were used to modify the AlBe foil surface. Air was excited in the chamber shown in figure 1. The separation between the plane foil anode and the tubular cathode was 12 mm. The RADAN-220 pulser was used as a pulsed voltage source. In the experiments, the discharge current amplitude was ∼3 kA with both polarities of the voltage pulse.

The total duration of the discharge current was ∼30 ns and the duration of the first half-period was ∼8 ns (figure 3(*b*)). With a negative polarity across the electrode of small curvature radius, the gas diode generated a runaway electron beam. With an electron energy higher than 50 keV and a beam current FWHM of ∼0.1 ns, the beam current amplitude was ∼10 A. The film was irradiated in the repetitive pulse mode with a pulse repetition frequency of 1 Hz. After the irradiation, the chemical composition of the film surface was examined by Auger spectroscopy.

Figure 10 shows the results of experiments on the discharge-induced surface modification of the AlBe foil. It is

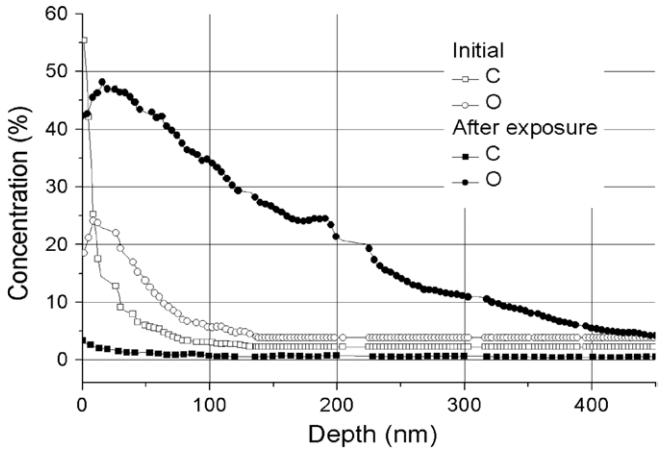


**Figure 10.** Carbon and oxygen concentration in relation to depth in near-surface layers of AlBe foil before and after the treatment with SAEB-induced diffuse discharge.

seen that the treatment with REP DD in atmospheric pressure air provides cleaning of the AlBe foil surface from carbon and an increase in oxygen concentration in the near-surface layers.

## 7. Conclusions

The nanosecond discharge in gaps filled with nitrogen, air and other gases in an inhomogeneous electric field was investigated. It is shown that decreasing the voltage pulse duration enhances the feasibility of a diffuse discharge with no additional ionization. The diffuse discharge is ignited due to the preionization of the gap by runaway electrons and x-ray quanta. With a negative polarity of the electrode of small curvature radius, the diffuse discharge develops due to preionization by the runaway electrons resulting from electric field amplification near the cathode and in the gap with the assistance of the positive ion charge. With a positive polarity of the electrode of small curvature radius, the x-rays generated by the runaway electrons decelerated in the gap and at the anode play an important part in the ignition of the diffuse discharge.

The REP DD has two characteristic stages. At the first stage, the ionization wave bridges the gap in a fraction of a second. The discharge current is determined by the conductivity of the dense plasma of the ionization wave and by the displacement current in the rest of the gap. The second discharge stage can be attributed to an anomalous glow discharge with a high specific input power. At the second stage, the voltage across the gap decreases and the cathode spots resulting from explosive electron emission can participate in the electron emission from the cathode. As the voltage pulse duration and specific input power are increased, the REP-to-spark discharge transition takes place.

The REP DD is readily realized in various gases and at different pressures. In the REP DD, the anode is affected by the dense plasma of the nanosecond discharge with a specific input power up to hundreds of megawatts per cubic centimetre, by the electron beam, shock wave and optical radiation of various spectral ranges, including UV and VUV, from the discharge plasma. This allows us to predict that the REP DD will find application in modification and cleaning of metal surfaces in different technological processes and, with a proper anode design, in modification and cleaning of dielectric surfaces. In helium, the decrease in pressure was found to increase the electron beam current downstream of the anode up to $\sim$2 kA cm$^{-2}$ [33]. The REP DD holds promise for design of high-power VUV excilamps. A similar discharge mode was used for ozone production [34]. We think that REP DDs will have widespread use in different fields.

## Acknowledgment

The authors are grateful to RFBR, project no 09-08-00030a, for partial support of the research.

## References

[1] McDaniel E W and Nighan W L (ed) 1982 *Gas Lasers* (New York: Academic)
[2] Mesyats G A, Osipov V V and Tarasenko V F 1995 *Pulsed Gas Laser* (Washington: SPIE Press)
[3] Endo I and Walter R F 2007 *Gas Lasers* (New York: CRC Press, Taylor and Francis Group)
[4] Noggle R C, Krider E P and Wayland J R 1968 *J. Appl. Phys.* **39** 4746
[5] Tarasova L V and Khudyakova L N 1969 *J. Tech. Phys.* **39** 1530
Tarasova L V and Khudyakova L N 1969 *Sov. Tech. Phys.* **14** 1148
[6] Babich L P and Lojko T V 1991 *J. Tech. Phys.* **61** 153
Babich L P and Lojko T V 1991 *Sov. J. Tech. Phys.* **61** 153
[7] Tarasova L V, Khudyakova L N, Loiko T V and Tsukerman V A 1974 *J. Tech. Phys.* **44** 564
Tarasova L V, Khudyakova L N, Loiko T V and Tsukerman V A 1975 *Sov. J. Tech. Phys.* **19** 351
[8] Babich L P 2003 *High-Energy Phenomena in Electric Discharges in Dense Gases: Theory, Experiment, and Natural Phenomena* (*ISTC Science and Technology Series* vol 2) (Arlington, VA: Futurepast)
[9] Tarasenko V F, Orlovskii V M and Shunailov S A 2003 *Russ. Phys. J.* **46** 325
[10] Alekseev S B, Gubanov V P, Kostyrya I D, Orlovskii V M and Tarasenko V F 2004 *Quantum Electron.* **34** 1007
[11] Tarasenko V F and Yakovlenko S I 2005 *Plasma Devices Oper.* **13** 231
[12] Kostyrya I D and Tarasenko V F 2004 *Russ. Phys. J.* **47** 1314
[13] Kostyrya I D, Orlovskii V M, Tarasenko V F, Tkachev A N and Yakovlenko S I 2005 *Tech. Phys. Lett.* **31** 457
[14] Bratchikov V B, Gagarinov K A, Kostyrya I D, Tarasenko V F, Tkachev A N and Yakovlenko S I 2007 *J. Tech. Phys.* **52** 856
[15] Repin P B and Rep'ev A G 2008 *Tech. Phys.* **53** 73
[16] Baksht E H, Rybka D V, Lomaev M I and Tarasenko V F 2006 *Quantum Electron.* **36** 576
[17] Lomaev M I, Mesyats G A, Rybka V D, Tarasenko V F and Baksht E H 2007 *Quantum Electron.* **37** 595
[18] Baksht E H, Burachenko A G, Lomaev M I, Rybka D V and Tarasenko V F 2008 *J. Tech. Phys.* **53** 93
[19] Tarasenko V F 2006 *Appl. Phys Lett.* **88** 081501
[20] Shulepov M A, Tarasenko V F, Goncharenko I M, Koval' N N and Kostyrya I D 2008 *Tech. Phys. Let.* **34** 296
[21] Krompholz H G, Hatfield L L, Neuber A A, Kohl K P, Chaporro J E and Ryu H 2006 *IEEE Trans. Plasma Sci.* **34** 927
[22] Baksht E H, Burachenko A G, Erofeev M V, Lomaev M I, Rybka D V, Sorokin D A and Tarasenko V F 2008 *Laser Phys.* **18** 732

[23] Baksht E H, Lomaev M I, Rybka D V, Sorokin D A and Tarasenko V F 2008 *Tech. Phys.* **53** 1560
[24] Tarasenko V F, Rybka D V, Baksht E H, Kostyrya I D and Lomaev M I 2008 *Instrum. Exp. Tech.* **51** 213
[25] Tarasenko V F, Baksht E H, Burachenko A G, Kostyrya I D, Lomaev M I and Rybka D V 2008 *Laser Part. Beams* **26** 605
[26] Kostyrya I D, Tarasenko V F and Schitz D V 2008 *Instrum. Exp. Techn.* **4** 159
[27] Yalandin M I, Shpak V G 2001 *Instrum. Exp. Techn.* **44** 285
[28] Tarasenko V F, Baksht E H, Burachenko A G, Kostyrya I D, Lomaev M I and Rybka D V 2008 *Plasma Devices Oper.* **16** 267
[29] Vasilyak L M, Kostyuchenko S V, Kudryavtsev N N and Filigyn I V 1994 *Usp. Fiz. Nauk.* **164** 263
Vasilyak L M, Kostyuchenko S V, Kudryavtsev N N and Filigyn I V 1994 *Phys.—Usp.* **37** 247
[30] Mesyats 2000 G A *Cathode Phenomena in a Vacuum Discharge: the Breakdown, the Spark and the Arc* (Moscow: Nauka)
[31] Askar'yan G A 1973 *Trudy FIAN* **66** 66
Askar'yan G A 1973 *Proc. P A Lebedev Phys. Inst. Acad. Sci. USSR* **66** 66
[32] Erofeev M V and Tarasenko V F 2008 *Quantum Electron.* **38** 401
[33] Baksht E H, Lomaev M I, Rybka D V and Tarasenko V F 2006 *Tech. Phys. Lett.* **32** 948
[34] Fukawa F, Shimomura N, Yano T, Yamanaka S, Teranishi K and Akiyama H 2008 *IEEE Trans. Plasma Sci.* **36** 2592